Hindawi
Advances in Civil Engineering
Volume 2019, Article ID 3073975, 12 pages
https://doi.org/10.1155/2019/3073975

Research Article

Damage Evolution Characteristics of Rock Salt under Different Stress Conditions

Chunping Wang[1,2] **Jianfeng Liu**[1] **and Lu Wang**[3]

[1]*State Key Laboratory of Hydraulics and Mountain River Engineering, Sichuan University, Chengdu, China*
[2]*CNNC Key Laboratory on Geological Disposal of High-Level Radioactive Waste, Beijing Research Institute of Uranium Geology, Beijing, China*
[3]*School of Civil Engineering, Architecture and Environment, Xihua University, Chengdu, China*

Correspondence should be addressed to Jianfeng Liu; ljfscu@163.com

Received 14 August 2019; Accepted 19 October 2019; Published 11 November 2019

Academic Editor: Eric Lui

Understanding the damage evolution characteristics of rock material is essential to the long-term stability and safety analysis of the underground facility. In this study, a series of cyclic loading tests under tensile or compressive stresses are conducted to investigate the damage evolution, deformation, peak strength, and failure pattern of rock salt. A special attention is paid on the microcracking process by using a 3D acoustic emission (AE) test system. The laboratory tests show that the damage degree of rock salt under compression is the highest, followed by the damage in the direct tensile test. The lowest value of damage is determined by using the Brazilian test. The damage degrees where the damage rate starts to decrease are about 0.83 in the direct tensile test, about 0.75 in the Brazilian test, and about 0.91 in the compression test. The failure mode of rock salt changes from the tensile mode in the uniaxial compression test to the compression-shear mode in the confined compression test at low confinement. But from the confining pressure of 15 MPa, the rock salt displays great plastic dilatant distortion and without appreciable macroscopic fractures. Accordingly, with increasing confining pressure, the positions where the rapid increase in cumulative AE counts occurs and where the AE event with high energy appears are changed, from the beginning of the test at low confinement to the postpeak stage of the test at high confinement.

1. Introduction

Because of the extremely low permeability [1, 2], excellent ductility [3, 4], good self-healing characteristics, and rheological response under stress [5–7], rock salt formations are commonly used as the geologic host rock for underground storage of natural gas, oil, petroleum, and compressed air and disposal of radioactive and other chemical wastes. Because of the disturbances from repeated drilling, blasting, and machinery transport during the excavation of underground constructions and the fluctuation of cavern pressures during the high-frequency of injection and withdrawal, the rock salt around storage caverns is usually subjected to a series of cyclic loadings [8–11]. The failure of rock under cyclic loading is a progressive fracturing process [12–15]. Therefore, it is of vital importance to investigate the effect of cyclic loading and the induced damage on the stability of salt cavern gas storage. A better understanding of the damage evolution characteristics of rock salt during the cyclic loading is essential to the design and long-term safety of the underground facility.

Over the last few decades, considerable effort has been put into studying the response of rock under cyclic uniaxial or triaxial loadings. Guo et al. [11] studied the mechanical properties of Jintan mine rock salt under complex stress paths based on a series of laboratory tests, including uniaxial compression, triaxial compression, unloading confining pressure, and cyclic loading tests. According to their research results, the axial strain of rock salt could be divided into three stages and the specimen had an instantaneous

collapse under the condition of cyclic loading. The effects of cyclic loading and the strain rate on the mechanical behavior of Chunar sandstone were analysed by Ray et al. [16]. The percentage decrease in uniaxial compressive strength was found to increase with the increase in the number of cycles. In addition, extensive investigations have been conducted to study the fatigue properties of rock material under cyclic loading [17–19]. It was reported that the cyclic loading led rock to fail at a lower fatigue strength [20].

Many research investigations focus on the compressive strength, elasticity, and time dependency under the effects of cyclic loadings [10, 21–23], the influence of the strain rate, confining pressure, temperature, and dynamic loading on the mechanical properties of rock [24–26], and also the stability and serviceability of storage caverns under cyclic loadings [27]. However, few studies explore the response of rock under different cyclic loadings and the corresponding development of damage. In this study, a series of cyclic loading tests under tensile or compressive stresses are conducted using the MTS815 rock mechanics test system. The objective was to investigate mechanical behavior of rock salt under different stress conditions and the corresponding damage characteristics. A 3D acoustic emission test system was used to monitor the microcracking process during the cyclic loading.

2. Laboratory Investigation

The rock salt samples adopted in the laboratory test are taken from a salt mine in Pingdingshan city, Henan Province of China. The samples are not homogeneity of NaCl (about 90%) but consist of anhydride, mudstone, or other impurities. Three types of specimens are prepared following the Standard for Test Method of Engineering Rock Mass [28], as presented in Figure 1. All the specimens in the Brazilian test have a diameter of 90 mm and a thickness of 45 mm. In the direct tensile test, cylindrical samples are used with a dimension of $\Phi 100\,\text{mm} \times H100\,\text{mm}$. Before the test, the specimen's two ends need to be bonded to two cylindrical steel caps through the high-strength adhesive. In uniaxial and confined compression tests, all specimens are processed into standard cylinders with the dimension of $\Phi 80\,\text{mm} \times H160\,\text{mm}$.

The MTS815 rock mechanics test system is used for the laboratory investigation, with a maximum axial loading capacity of 4600 kN and a maximum confining pressure of 140 MPa. The linear variable differential transformer (LVDT) can be installed on the machine to measure the axial displacement of the rock sample. According to the testing method suggested by China standard [28], two steel bars are placed between the flat steel plate and the disc specimen in the Brazilian test to provide a symmetric line loading. The test is performed in a strain control mode, with an axial LVDT displacement rate of 0.3 mm/min. In the direct tensile test, a testing apparatus named the device with the position-limit spring for the alternating tension-compression cyclic test [29], which is developed by our research team, is used. The maximum uniaxial tensile load can reach 2300 kN. Previous studies show that the device can be easily applied for investigating the tensile behavior of rock salt [30]. The direct tensile test can be performed with either a stress or a strain control mode. In this study, the loading is controlled by the axial LVDT displacement rate, which is 0.01 mm/min at the beginning of the test and then decreased to 0.001 mm/min when the increasing stress is about 80% of the experiential peak strength of rock salt. In the triaxial compression test, the confining pressures of 5, 10, 15, 20, 30, and 40 MPa are applied. In order to determine the damage evolution characteristics during the failure process of rock salt, the loading-unloading cycles are performed at different stress levels in any of the tests. The triaxial compression test is performed with a stress control mode, at a constant loading rate of 3 MPa/min for confining pressure and 30 kN/min for axial force. The unloading rate of axial force is 60 kN/min. All the tests are conducted at room temperature (25°C), and the loading time of each specimen is about half an hour to one half.

Based on a 3D acoustic emission test system, the microcracking process during the cyclic loading is recorded. 8 Mic30 AE sensors are used in the three types of tests with a central frequency 300 kHz and a preamplifier gain of 40 dB. Waveform parameters, including energy, counts, amplitude, duration, rise time, and average frequency, are captured and calculated. Based on the arrival times of the first wave at each sensor and their respective velocity in the rock specimen, the location of the AE events can be estimated by the least-square method. For a measurable event, a minimum of four arrived times is needed.

3. Experimental Results

The tensile strength and triaxial compression strength of rock salt are presented in Table 1. In the direct tensile test, the rock specimen is under a simple uniaxial tensile stress condition, and the rock failure generally occurs at the most vulnerable part of the specimen. Thus, the tensile strength determined from the direct tensile test is more reliable and genuine. However, there are high requirements for the experimental set-up and samples in the direct tensile test. For instance, the axial lines of the testing machine, the measurement device, and the specimen should be aligned. The two end surfaces should be parallel and perpendicular to the axial line of the specimen. Consequently, the easier indirect tensile method, such as the Brazilian test, is widely used. But because the disc specimen in the Brazilian test is under a complicated stress condition coupling with tensile and compressive stress, the tensile strength determined by the Brazilian test may be different from that determined by the direct tensile test. In this study, the average tensile strength determined by the Brazilian test is 1.65 MPa, which is about 17% higher than the average tensile strength determined by the direct tensile test (1.41 MPa). These results may be attributed to the end restraint effect induced by the large contact surface between the plate and the specimen in the Brazilian test, which may restrict the development of the tensile fracture and lead to a relatively higher tensile strength.

3.1. Tensile Test. There are many forms to define the damage of rock material. In the laboratory test, the damage of the

(a) (b) (c)

Figure 1: Illustration of rock samples for different tests. (a) Sample for the Brazilian test. (b) Sample for the direct tensile test. (c) Sample for the compression test.

Table 1: Experimental results from different tests.

Experimental type	Sample	Confining pressure (MPa)	Peak strength (deviatoric stress, MPa)
Direct tensile test	T-1	—	1.33
	T-2	—	1.42
	T-3	—	1.48
Brazilian test	B-1	—	1.56
	B-2	—	1.62
	B-3	—	1.79
Compression test	C-1	0	21.58
	C-2	5	52.67
	C-3	10	55.75
	C-4	15	59.29
	C-5	20	63.81
	C-6	30	63.57
	C-7	40	63.93

rock sample is generally defined as the deterioration degree of the elastic modulus [31, 32]. Ju and Xie proposed an improved method by considering the effect of the irreversible plastic deformation [33]. The damage can be expressed as follows:

$$D = 1 - \left(1 - \frac{\varepsilon_p}{\varepsilon}\right)\frac{E^{\%}}{E}, \quad (1)$$

where ε is the total strain at the beginning of unloading, ε_p is the residual inelastic strain at the end of unloading, E is the initial and undamaged elastic modulus, and $E^{\%}$ is the reduced modulus in unloading. Considering that rock salt has significant inelastic deformation, in this study, we continue to use the aforementioned equation to calculate the damage of rock salt under different stress conditions.

Figure 2 shows the stress-strain curves in the direct tensile test (Figure 2(a)) and Brazilian test (Figure 2(b)) and the corresponding evolution process of damage and inelastic strain. The deformation at peak stress in the Brazilian test is noticed to be higher than that in the direct tensile test. It is because the deformation in the Brazilian test is induced not only by the tensile fracture at the center of the disc specimen but also by the compression-tensile fracture at the contact surface between the flat plate and the specimen. The damages in the direct tensile test and Brazilian test both experience a process of rapid increasing first at low-stress levels and, then, slow increasing when the damage accumulates to some extent. The damage degree where the damage rate starts to decrease is about 0.83 in the direct tensile test when the stress level is about 50% of the peak stress and is about 0.75 in the Brazilian test when the stress level is about 25% of the peak stress.

Figures 2(c) and 2(d) show the damage evolution process in the direct tensile test and Brazilian test, respectively. For the rock specimens in the same experimental condition, a similar tendency of damage evolution can be noticed. On the whole, the level of damage in the direct tensile test is higher than that in the Brazilian test. It can be attributed to the failure mode of the rock specimen. In the direct tensile test, the rock failure generally occurs quickly at the most vulnerable part of the specimen with a small axial strain. In the Brazilian test, however, the disc specimen is not completely split after peak stress and still has a certain bearing capacity. Accordingly, the damage degree is relatively lower.

At the end of each unloading, an inelastic deformation can be observed on rock salt. Figures 2(e) and 2(f) show the inelastic strain at the end of each unloading in the direct tensile test and Brazilian test. The inelastic strain is found to

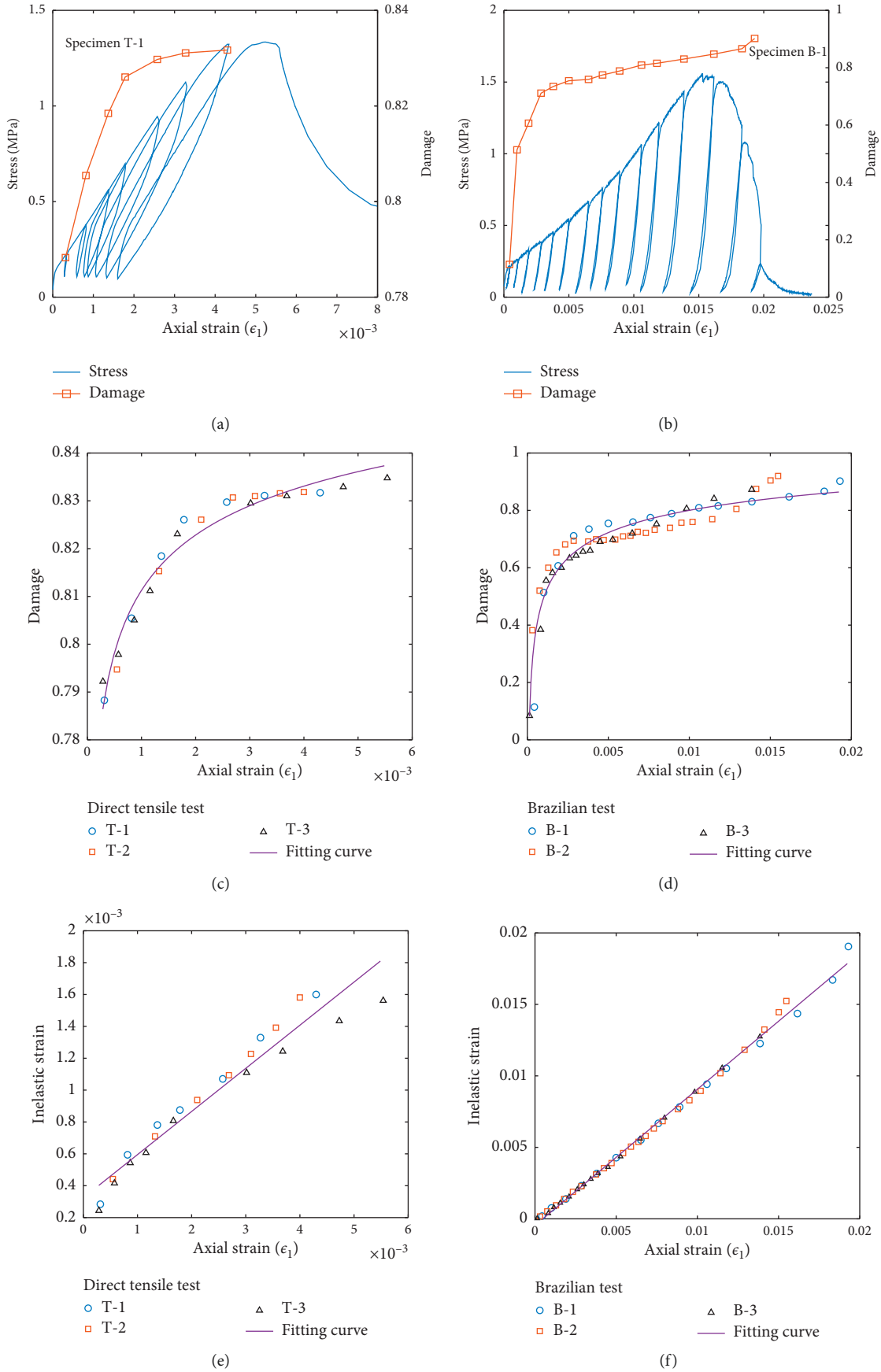

Figure 2: Stress-strain curves and the evolution process of damage and inelastic strain during the direct tensile test and Brazilian test.

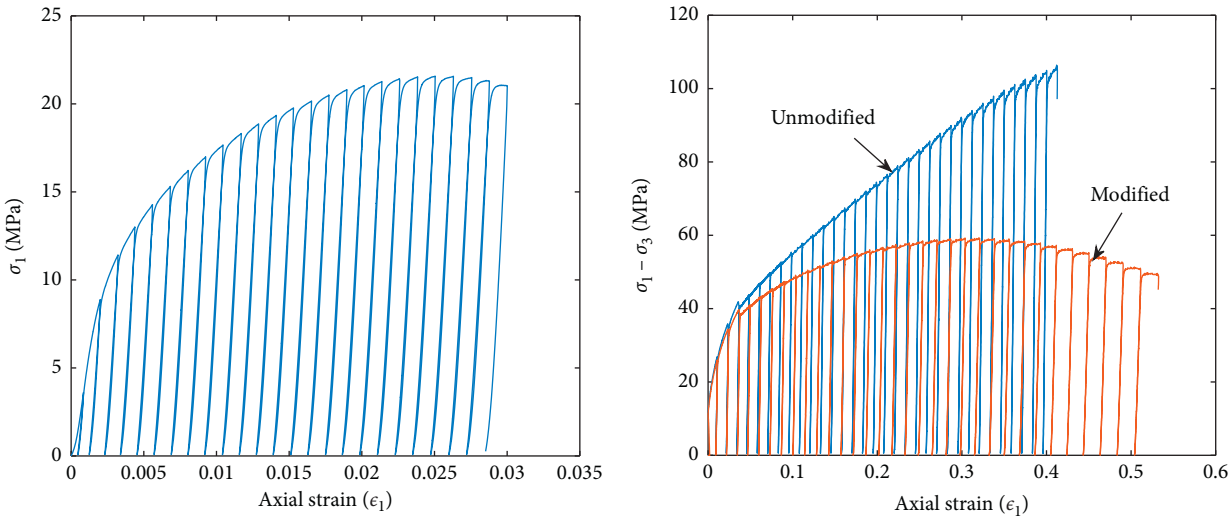

Figure 3: Stress-strain curves of rock salt in the compression test. (a) $\sigma_3 = 0$ MPa. (b) $\sigma_3 = 15$ MPa.

increase linearly with increasing axial strain. The inelastic strain in the direct tensile test is much lower than that in the Brazilian test. The recoverable elastic strain of the rock specimen during each loading-unloading cycle in the Brazilian test is very limited.

3.2. Compression Test. There are generally two typical ways to describe the strain of rock, namely engineering strain and logarithmic strain. The engineering strain is the ratio of the variation of specimen's height to the initial height of the specimen. The logarithmic strain means the sum of the increment of strain under the same principal axis of strain, which can describe the true state of the specimen's deformation. When the deformation of the rock specimen is small, the calculated engineering strain is close to the result of logarithmic strain. However, in the case of large deformation, great errors may be induced by engineering strain. In the triaxial compression test on rock salt, there will be large compressive deformation in axial direction, especially when the confining pressure is higher than 15 MPa [34]. The increase in the cross-sectional area is particularly apparent. Therefore, the logarithmic strain is used in this study to describe the variation of strain of rock salt in the triaxial stress state. Meanwhile, the cross-sectional area is modified to calculate the axial stress.

Figure 3 shows the stress-strain curves of rock salt in the uniaxial compression test and triaxial compression test with a confining pressure of 15 MPa. The axial strain in the uniaxial compression test is relatively small. At confining pressure of 15 MPa, the unmodified axial stress shows hardening characteristics with increasing axial strain. Accordingly, the peak stress cannot be determined. After using the logarithmic strain to modify the axial strain and axial stress of rock salt, the softening characteristic of axial stress appears with an evident peak stress.

The modified compressive strain and stress of rock salt under different confining pressures are obtained (Table 1). Figure 4 shows the envelopes of the modified stress-strain curves and the peak strengths at different confinements. The variation of compressive strength with confining pressure can be fit well with the Hou/Lux model [35] given as follows:

$$\beta^{\mathrm{TC}}(\sigma_3) = a_6 - a_7 \exp(-a_8 \sigma_3), \tag{2}$$

where σ_3 is the confining pressure and a_6, a_7, and a_8 can be determined from the curve fitting of test results. In this study, a_6, a_7, and a_8 are 62.75, 40.79, and 0.24, respectively. The compressive strength of rock salt is found to be increased with increasing confinement when confining pressure is lower than 10 MPa. The increment is most significant when confining pressure is increased from 0 to 10 MPa. The unconfined compressive strength of rock salt is 21.58 MPa. Changes of the compressive strengths are fairly minor when increasing the confining pressure from 15 MPa to 40 MPa. Consequently, we speculate that there may be a critical confining pressure between 10 MPa and 15 MPa, under which the mechanical behavior of rock salt maybe changed. This speculation may be verified by the failure patterns of rock salt under different confining pressures, which will be discussed in Section 4.

Figure 5 shows the evolution process of damage and inelastic strain under different confining pressures. It is interesting to find that although the confining pressure is different, the development of damage and also the variation of inelastic strain of different rock specimens are the same. When the axial strain of rock salt is developed to the same level, a similar damage and inelastic strain can be observed for rock specimens at different confining pressures. There is a critical axial strain for rock salt at which the growth rate of damage becomes slow from rapid. For rock salt in this study, the critical axial strain is about 0.05.

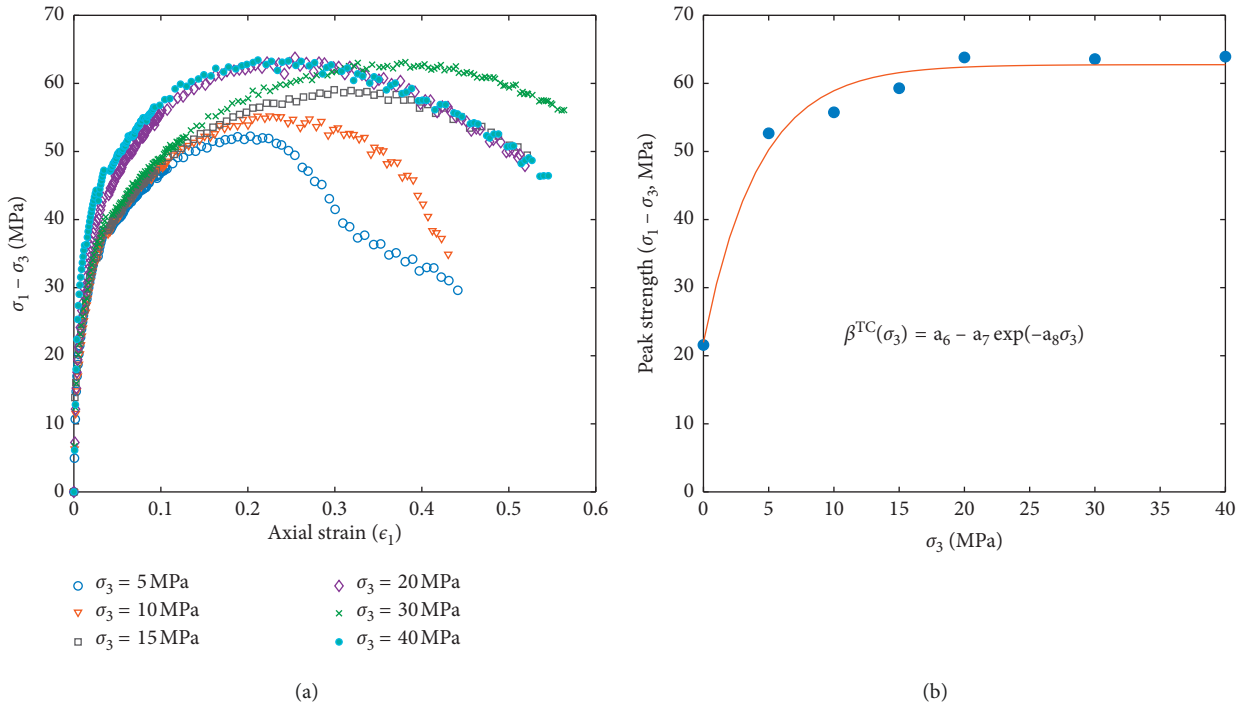

FIGURE 4: Stress-strain curves and peak strength of rock salt at different confining pressures. (a) Stress-strain curves. (b) Peak strength at different confinements.

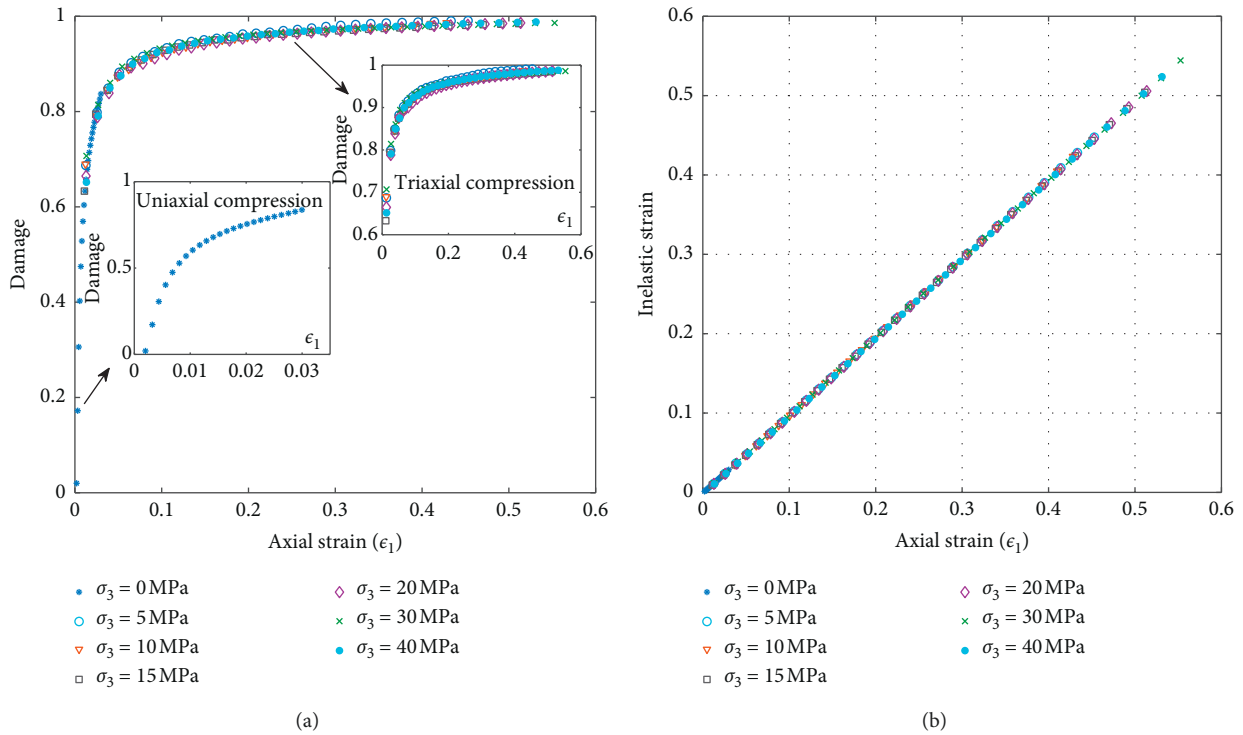

FIGURE 5: Evolution processes of damage and inelastic strain at different confinements. (a) Damage evolution process. (b) Variation of inelastic strain.

From equation (1), the damage degree depends not only on the degradation of the elastic modulus but also on the accumulation of inelastic strain. For rock salt under compression, the inelastic strain is relatively high, especially under triaxial compression. The accumulation of inelastic strain may dominate the develop of damage. Accordingly,

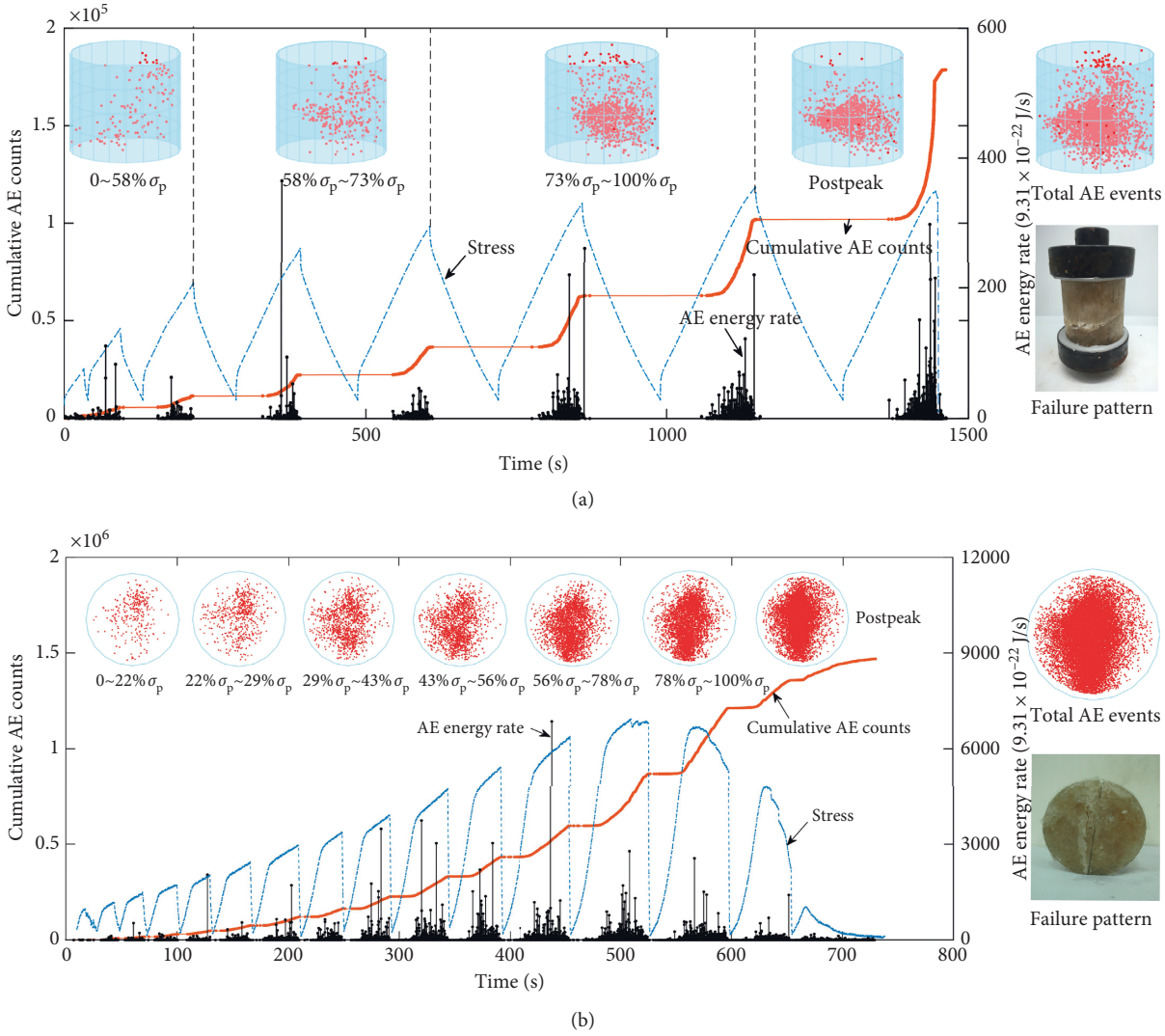

FIGURE 6: Evolution of AE characteristics (cumulative AE counts, AE energy rate, and spatial distribution of AE events) and failure patterns in tensile tests. (a) Direct tensile test (T-2). (b) Brazilian test (B-1).

the damage degree in the compression test is relatively higher than that in the tensile test. The recoverable elastic strain in one cycle of loading-unloading is very limited, which is similar to the Brazilian test.

4. Acoustic Emission Characteristics

As an economic and efficient nondestructive testing method, acoustic emission technology is widely used in laboratories and fields to study the damage evolution process of rock materials. In this study, a 3D acoustic emission testing system is used in both tensile and compression tests. Based on the arrival times of the first wave at each sensor and their respective velocity in the rock specimen, the location of each AE event is evaluated.

Figure 6 shows the variation of cumulative AE counts and AE energy rates during the tensile test and also the spatial distribution of AE events at different stress stages. The growth in cumulative AE counts mainly takes place at the stress loading stage. When the stress level is lower than the maximum stress of the previous cycle or the rock specimen is in stress unloading stage, almost no AE events are detected. In the low-stress stage (<58% σ_p, σ_p is the peak stress) of the direct tensile test (Figure 6(a)), the AE events are dispersedly distributed inside the specimen and the number of AE events is very limited. The increase in cumulative AE counts is slow, and the energy of the AE event is relatively low. And until the stress level is up to 73% σ_p, a large number of AE events with high energy can be detected. The number of cumulative AE counts increases rapidly, and the AE events mainly occur at the failure surface of the rock specimen. The specimen is not completely fractured at the peak stress stage and still has certain tensile capacity. In the postpeak stage, there are still lot of AE events gathered along the macroscopic failure surface. At the beginning of the Brazilian test (Figure 6(b)), many AE events with low energy are observed to be widely distributed inside the specimen, which can be attributed to the closure of the intrinsic microcracks. From about 56% of

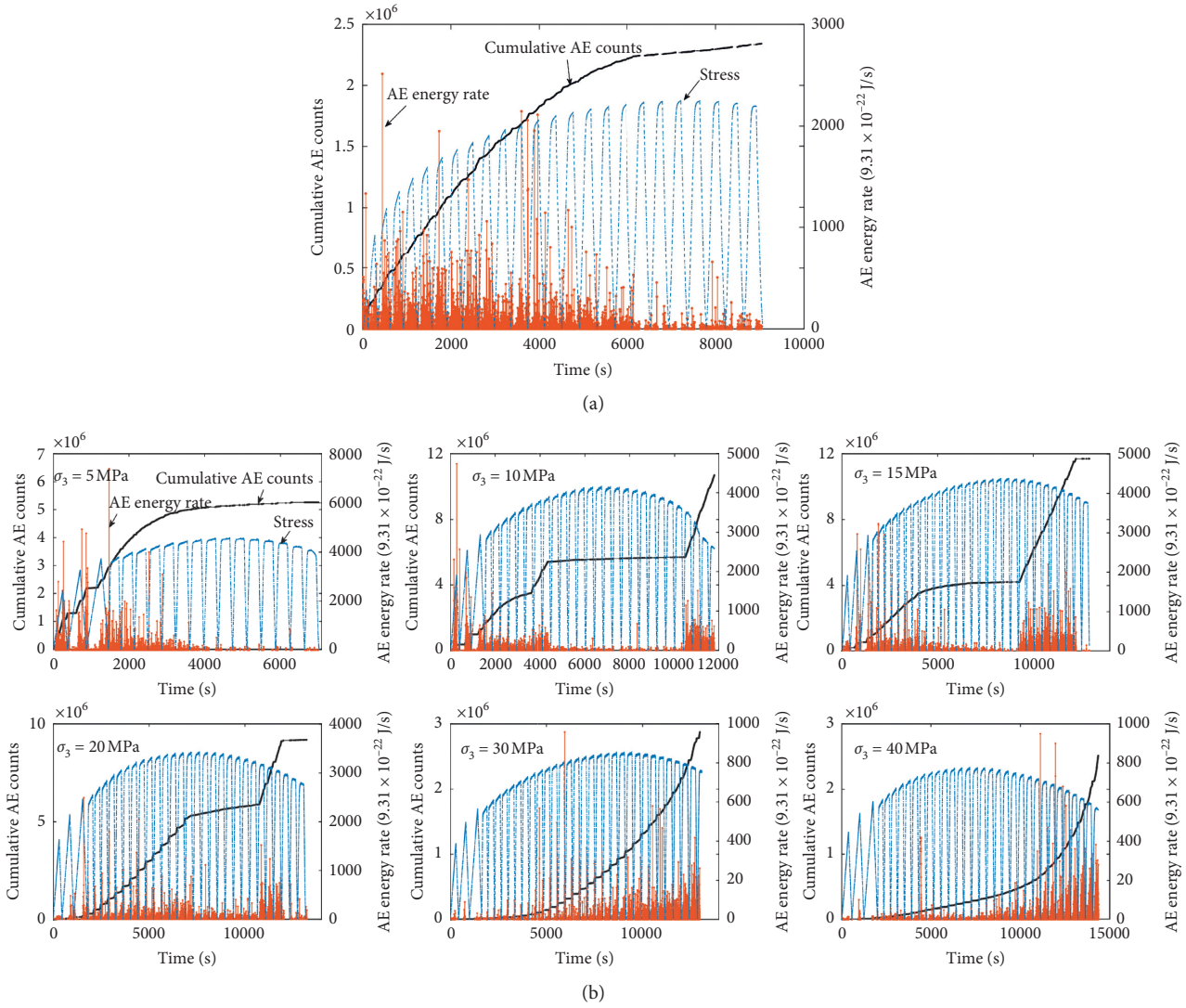

Figure 7: Variations of cumulative AE counts and AE energy rates in compression tests. (a) Uniaxial compression test. (b) Triaxial compression test.

the peak stress, the concentration of AE events along the failure surface becomes apparent. The energies of those AE events are generally higher. When the stress level is close to the peak stress, the increase in cumulative AE counts is accelerated. Similar to the direct tensile test, the disc specimen still has abundant capacity of compression-tensile deformation in the postpeak stage. Although many AE events still can be detected, the growth of cumulative AE counts is slowing.

Figure 7 shows the variation of cumulative AE counts and AE energy rates in the compression test. It can be noticed that, at high confinement, the positions where the rapid increase in cumulative AE counts occurs and where the AE event with high energy appears are different from those at low confinement. In the uniaxial compression test and triaxial compression test under a confining pressure of 5 MPa, a great deal of AE events with high energy are detected at the beginning of the test. The cumulative AE counts are growing fast. But when the stress level is near the peak stress, the AE energy rate obviously drops and the growth rate of the cumulative AE counts slows down. Under confining pressures of 10 MPa, 15 MPa, and 20 MPa, a great increase in cumulative AE counts also can be observed in the postpeak stage of the test besides the beginning of the test. The corresponding AE events also have a relatively high energy. The higher the confining pressure is, the less time the low growth in cumulative AE counts experiences. When the confining pressure is increased to 30 MPa or 40 MPa, the number of AE events at the beginning of the test is very limited, and the corresponding energy is relatively low. From about 85% of the peak stress, a large number of AE events with high energy start to be detected. In addition, under a confining pressure of 40 MPa, the growth rate of cumulative AE counts is accelerated again at about 90% of the peak stress in the postpeak stage.

In order to give a better understanding of the acoustic emission characteristics during the compression test, the spatial distribution of AE events at different stress levels is

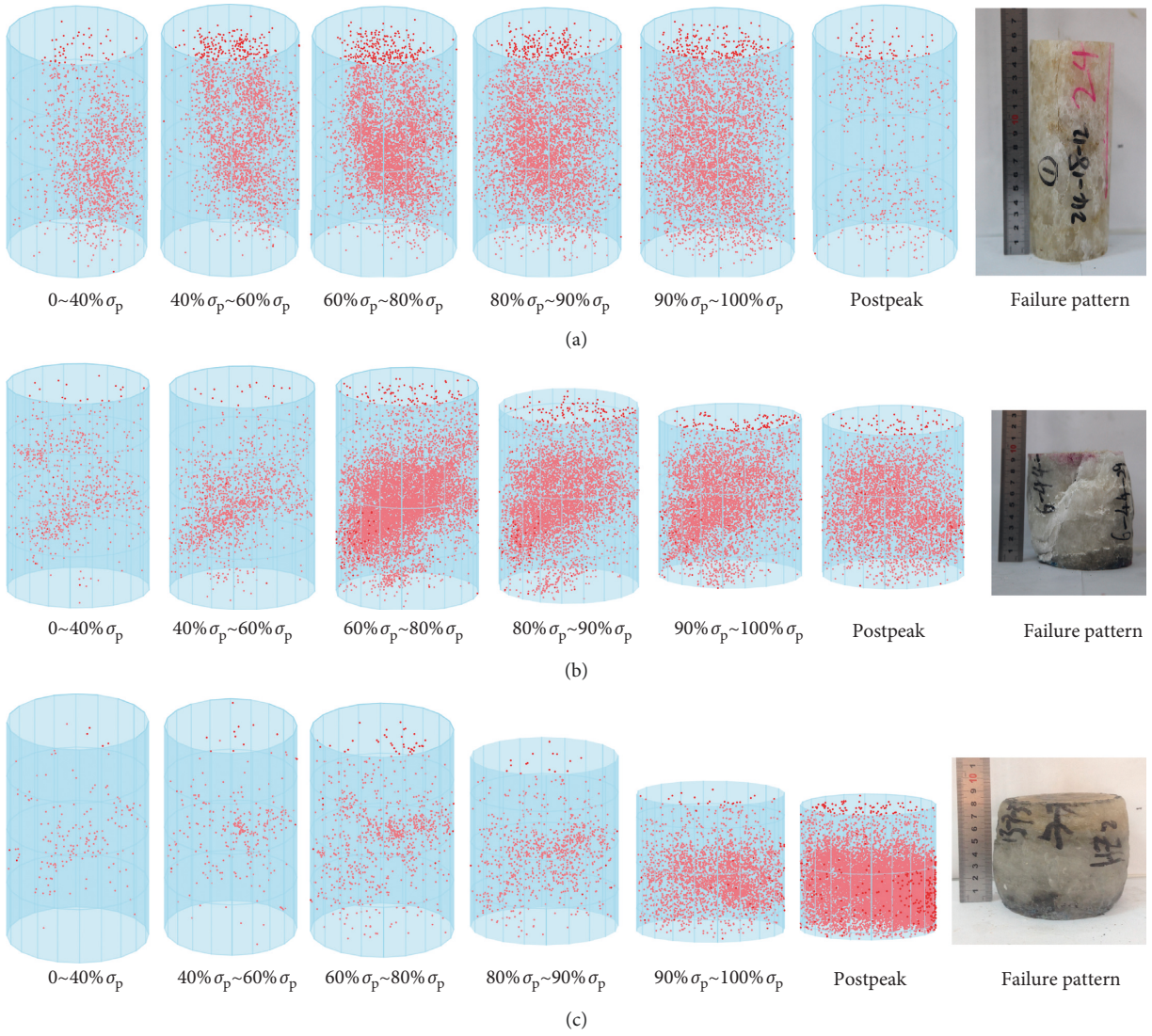

Figure 8: Spatial distribution of AE events and failure patterns of rock salt at different confining pressures. (a) $\sigma_3 = 0$ MPa. (b) $\sigma_3 = 10$ MPa. (c) $\sigma_3 = 40$ MPa.

presented in Figure 8. Consistent with the curve of cumulative AE counts, the AE events mainly occur at the stage of 60%σ_p~100%σ_p (σ_p is the peak stress) at low confinement, and in the postpeak stage at high confinement. In the uniaxial compression test, many AE events are detected under low stress, which can be attributed to the closure of the intrinsic microcracks inside the specimen. With the increasing stress level, new microcracks are induced and propagate to macroscopic cracks, accompanied by AE events. In the triaxial compression test, some intrinsic microcracks become closed during the loading stage of confining pressure. Accordingly, in the low-stress stage before the formation of new microcracks, the number of AE events is relatively limited. In addition, the higher the confining pressure, the less the number of AE events in the low-stress stage.

Figure 9 shows the spatial distribution of AE events with different amplitudes in the tensile test and compression test. Combining with the failure patterns of rock salt under different confining pressures in Figure 10, it can be noticed that the AE events especially those with high energy amplitude are mainly concentrated at the final failure surface of the rock specimen. Generally, the AE event with high amplitude means microcracking accompanied by the release of high elastic energy; that is, the released energy of the cracks near the failure surface is generally higher. This is especially apparent in the tensile test and uniaxial compression test. In the uniaxial compression test, the failure mode of rock salt is tensile failure with multiple fracture surfaces along the axial direction. The final deformation of the rock specimen is small. In the confined compression test with low confining pressures, the rock specimen shows a compression-shear failure mode with significant axial deformation and lateral deformation. When the confining pressure is higher than 15 MPa, the rock specimen displays great plastic dilatant distortion and is full of widely distributed microcracks.

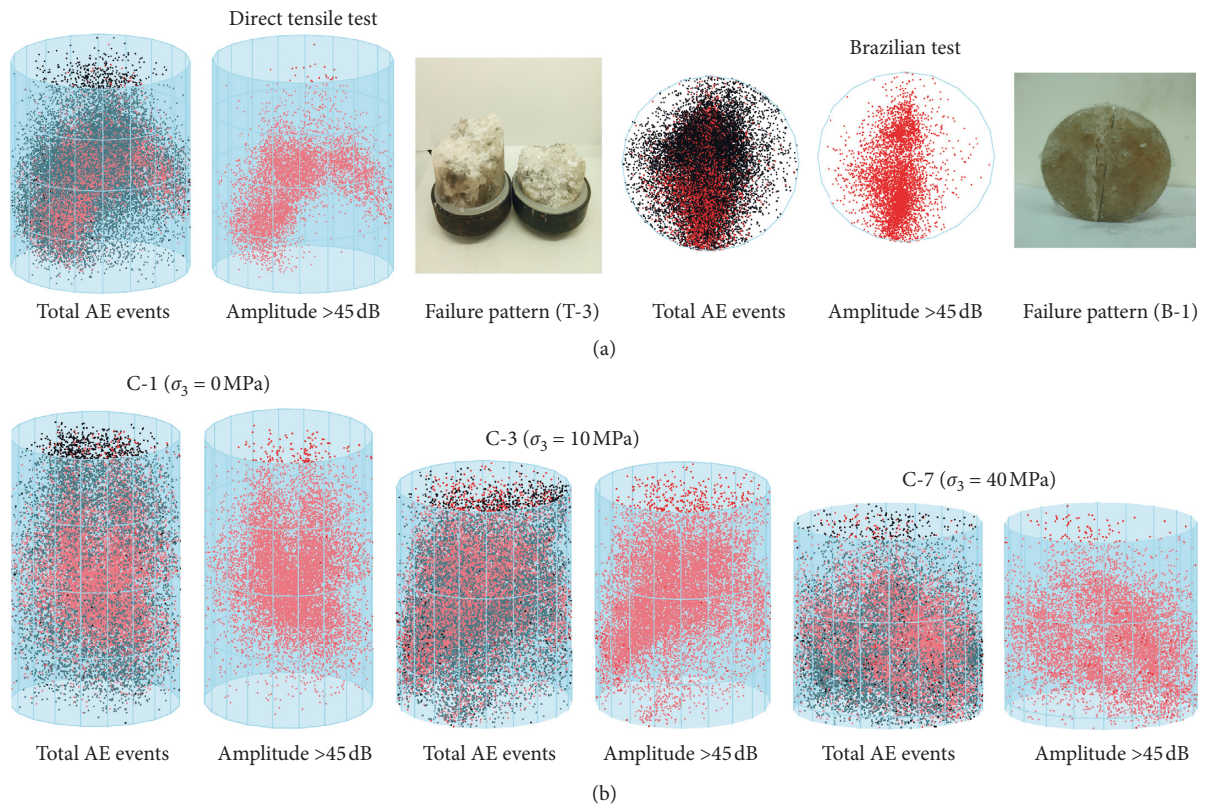

Figure 9: Spatial distributions of total AE events and AE events with amplitude >45 dB. (a) Tensile test. (b) Compression test.

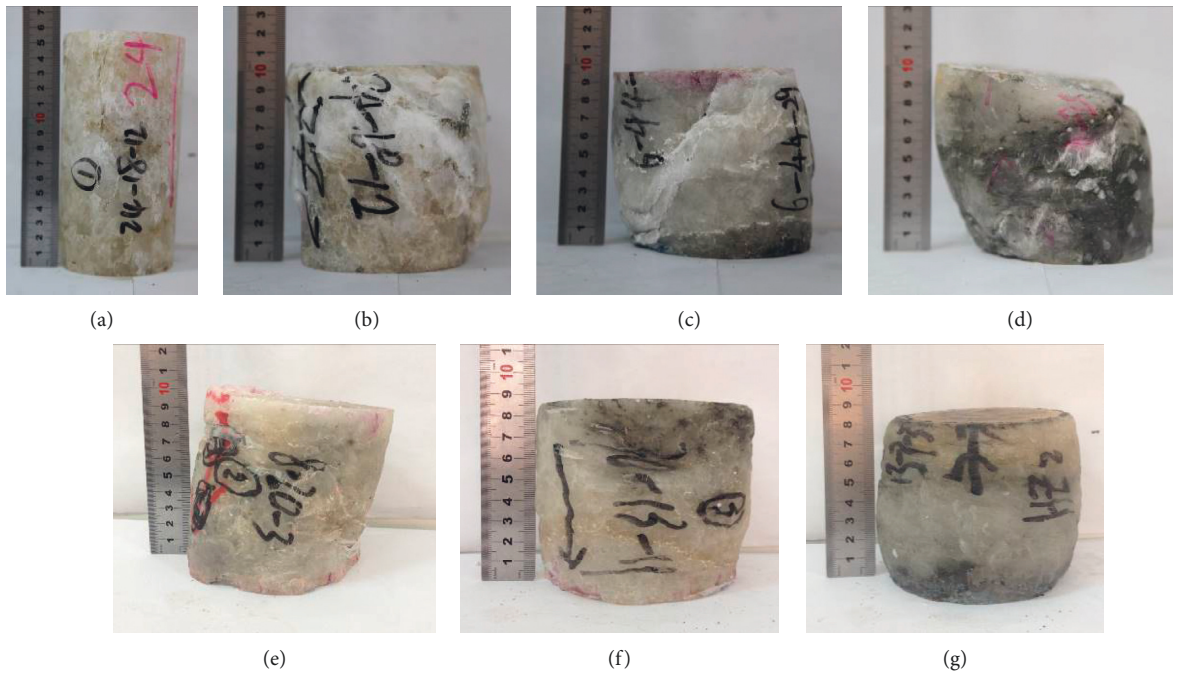

Figure 10: Failure patterns of rock salt under different confining pressures. (a) $\sigma_3 = 0$ MPa. (b) $\sigma_3 = 5$ MPa. (c) $\sigma_3 = 10$ MPa. (d) $\sigma_3 = 15$ MPa. (e) $\sigma_3 = 20$ MPa. (f) $\sigma_3 = 30$ MPa. (g) $\sigma_3 = 40$ MPa.

5. Discussion and Conclusions

Based on the MTS815 rock mechanics test system and 3D acoustic emission test system, the mechanical behavior of rock salt and damage evolution characteristics under different stress conditions are studied. First, the tensile strength of rock salt determined by the Brazilian test is about 17% higher than that determined by using the direct tensile test. Despite the good accuracy of the direct tensile test, the laboratory test has high requirements for the experimental set-up and samples. Different from the direct tensile test, the rock specimen in the Brazilian test is not under a simple uniaxial tensile stress state, which leads to a small deviation in tensile strength and deformation. The deformation is induced not only by the tensile fracture at the center of the disc specimen but also by the compression-tensile fracture at the contact surface between the flat plate and specimen.

In the compression test, there is an apparent increase in compressive strength by increasing the confining pressure from 0 to 10 MPa. But changes of the compressive strengths are fairly minor when increasing the confinement from 15 MPa to 40 MPa. Similarly, the failure pattern of rock salt at high confinement is quite different from that at low confinement (Figure 10). At low confinement ($\sigma_3 < 15$ MPa), the rock specimens have one or more apparent fracture surfaces. The failure mode changes from the tensile mode in the uniaxial compression test to the compression-shear mode in the confined compression test. But from a confining pressure of 15 MPa, the rock salt displays great plastic dilatant distortion and without appreciable macroscopic fractures. Based on the previous analysis, we speculate that there may be a critical confining pressure between 10 MPa and 15 MPa, under which the mechanical behavior of rock salt may be changed. And a series of compression tests at confinement from 10 MPa to 15 MPa will be further conducted to verify this speculation.

Based on equation (1), the damage of rock salt under different stress states is calculated. The damages in three different types of tests all experience a process of rapid increasing first at low-stress levels and, then, slow increasing when the damage accumulates to some extent. The damage degrees where the damage rate starts to decrease are about 0.83 in the direct tensile test when the stress level is about 50% of the peak stress and about 0.75 in the Brazilian test when the stress level is about 25% of the peak stress. When the damage degree accumulates to 0.91 in the compression test, the damage rate becomes slow at a critical axial strain of 0.05. For the three different types of tests in this study, the damage degree of rock salt under compression is the highest, followed by the damage in the direct tensile test. The lowest value of damage is determined from the Brazilian test.

A distinct Kaiser effect can be observed in the tensile test. When the stress level is lower than the maximum stress of the previous cycle or the rock specimen is in the stress unloading stage, almost no AE events are detected. In the compression test, with increasing confining pressure, the positions where the rapid increase in cumulative AE counts occurs and where the AE event with high energy appears are changed, from the beginning of the test at low confinement to the postpeak stage of the test at high confinement. This change maybe attributed to the differences of failure modes of rock salt under different confining pressures.

These findings may be somewhat limited by the range of confining pressures; nevertheless, the findings have a certain significance for understanding the mechanical properties of rock salt and the damage evolution characteristics under different stress conditions. A number of possible studies on rock salt using a similar experimental approach with a wider range of confining pressures will be performed in the future.

Data Availability

The data used to support the findings of this study are available from the corresponding author on request.

Conflicts of Interest

The authors declare that they have no conflicts of interest.

Acknowledgments

This work has been supported by the National Natural Science Foundation of China (no. 51874202) and Sichuan Youth Science and Technology Fund (no. 2017JQ0003). The authors wish to offer their gratitude and regards to the colleagues who contributed to this article.

References

[1] J. C. Stormont and J. J. K. Daemen, "Laboratory study of gas permeability changes in rock salt during deformation," *International Journal of Rock Mechanics and Mining Sciences*, vol. 29, no. 4, pp. 325–342, 1992.

[2] H. Alkan, Y. Cinar, and G. Pusch, "Rock salt dilatancy boundary from combined acoustic emission and triaxial compression tests," *International Journal of Rock Mechanics and Mining Sciences*, vol. 44, no. 1, pp. 108–119, 2007.

[3] U. Hunsche, "Fracture experiments on cubic rock salt samples," in *Proceedings of the 1st International Mechanical Behavior of Salt Conference*, pp. 169–179, State College, PA, USA, November 1981.

[4] C. J. Spiers, C. J. Peach, R. H. Brzesowsky, P. M. Schutjens, J. L. Liezenberg, and H. J. Zwart, *Long Term Rheological and Transport Properties of Dry and Wet Salt Rocks. Final Report*, University of Utrecht, Utrecht, The Netherlands, 1988.

[5] S. Bachu and W. D. Gunter, "Storage capacity of CO_2 in geological media in sedimentary basins, with application to the Alberta Basin," in *Proceedings of the 4th International Conference on Greenhouse Gas Control Technology (GHGT-4)*, Elsevier, Interlaken, Switzerland, August 1998.

[6] S. Bachu and L. Rothenburg, "Carbon dioxide sequestration in salt caverns: capacity and long term fate," in *Proceedings of the 2nd Annual Conference on Carbon Dioxide Sequestration (CD-ROM)*, p. 12, Alexandria, VA, USA, May 2003.

[7] M. B. Dusseault, L. Rothenburg, and S. Bachu, "Sequestration of CO_2 in salt caverns," in *Proceedings of the Canadian International Petrol Conference (CD-ROM)*, Calgary, Alberta, Canada, June 2002.

[8] J. Liu, H. Xie, Z. Hou, C. Yang, and L. Chen, "Damage evolution of rock salt under cyclic loading in unixial tests," *Acta Geotechnica*, vol. 9, no. 1, pp. 153–160, 2014.

[9] L. Blanco-Martín, A. Rouabhi, J. Billiotte et al., "Experimental and numerical investigation into rapid cooling of rock salt related to high frequency cycling of storage caverns," *International Journal of Rock Mechanics and Mining Sciences*, vol. 102, pp. 120–130, 2018.

[10] L. J. Ma, X. Y. Liu, M. Y. Wang et al., "Experimental investigation of the mechanical properties of rock salt under triaxial cyclic loading," *International Journal of Rock Mechanics and Mining Sciences*, vol. 62, no. 9, pp. 34–41, 2013.

[11] Y. Guo, C. Yang, and H. Mao, "Mechanical properties of Jintan mine rock salt under complex stress paths," *International Journal of Rock Mechanics and Mining Sciences*, vol. 56, pp. 54–61, 2012.

[12] C. D. Martin and N. A. Chandler, "The progressive fracture of Lac Du Bonnet granite," *International Journal of Rock Mechanics and Mining Sciences & Geomechanics Abstracts*, vol. 31, no. 6, pp. 643–659, 1994.

[13] E. Eberhardt, D. Stead, and B. Stimpson, "Quantifying progressive pre-peak brittle fracture damage in rock during uniaxial compression," *International Journal of Rock Mechanics and Mining Sciences*, vol. 36, no. 3, pp. 361–380, 1999.

[14] S. L. Qiu, X. T. Feng, J. Q. Xiao, and C. Q. Zhang, "An experimental study on the pre-peak unloading damage evolution of marble," *Rock Mechanics and Rock Engineering*, vol. 47, no. 2, pp. 401–419, 2014.

[15] J. W. Fu, X. Z. Zhang, W. S. Zhu, K. Chen, and J. F. Guan, "Simulating progressive failure in brittle jointed rock masses using a modified elastic-brittle model and the application," *Engineering Fracture Mechanics*, vol. 178, pp. 212–230, 2017.

[16] S. K. Ray, M. Sarkar, and T. N. Singh, "Effect of cyclic loading and strain rate on the mechanical behaviour of sandstone," *International Journal of Rock Mechanics and Mining Sciences*, vol. 36, no. 4, pp. 543–549, 1999.

[17] J.-Q. Xiao, D.-X. Ding, F.-L. Jiang, and G. Xu, "Fatigue damage variable and evolution of rock subjected to cyclic loading," *International Journal of Rock Mechanics and Mining Sciences*, vol. 47, no. 3, pp. 461–468, 2010.

[18] N. Li, P. Zhang, Y. Chen, and G. Swoboda, "Fatigue properties of cracked, saturated and frozen sandstone samples under cyclic loading," *International Journal of Rock Mechanics and Mining Sciences*, vol. 40, no. 1, pp. 145–150, 2003.

[19] M. N. Bagde and V. Petroš, "Fatigue properties of intact sandstone samples subjected to dynamic uniaxial cyclical loading," *International Journal of Rock Mechanics and Mining Sciences*, vol. 42, no. 2, pp. 237–250, 2005.

[20] M. N. Bagde and V. Petroš, "Fatigue and dynamic energy behaviour of rock subjected to cyclical loading," *International Journal of Rock Mechanics and Mining Sciences*, vol. 46, no. 1, pp. 200–209, 2009.

[21] K. Fuenkajorn and D. Phueakphum, "Effects of cyclic loading on mechanical properties of Maha Sarakham salt," *Engineering Geology*, vol. 112, no. 1–4, pp. 43–52, 2010.

[22] Y. T. Guo, K. L. Zhao, G. H. Sun, C. H. Yang, H. L. Ma, and G. M. Zhang, "Experimental study of fatigue deformation and damage characteristics of salt rock under cyclic loading," *Chin J Rock Soil Mech*, vol. 32, no. 5, pp. 1353–1359, 2011.

[23] W. Liang, C. Zhang, H. Gao, X. Yang, S. Xu, and Y. Zhao, "Experiments on mechanical properties of salt rocks under cyclic loading," *Journal of Rock Mechanics and Geotechnical Engineering*, vol. 4, no. 1, pp. 54–61, 2012.

[24] N. Li, W. Chen, P. Zhang, and G. Swoboda, "The mechanical properties and a fatigue-damage model for jointed rock masses subjected to dynamic cyclical loading," *International Journal of Rock Mechanics and Mining Sciences*, vol. 38, no. 7, pp. 1071–1079, 2001.

[25] S. W. Zhou, C. C. Xia, Y. S. Hu, Y. Zhou, and P. Y. Zhang, "Damage modeling of basaltic rock subjected to cyclic temperature and uniaxial stress," *International Journal of Rock Mechanics and Mining Sciences*, vol. 77, pp. 163–173, 2015.

[26] A. Y. Cao, G. C. Jing, Y. L. Ding, and S. Liu, "Mining-induced static and dynamic loading rate effect on rock damage and acoustic emission characteristic under uniaxial compression," *Safety Science*, vol. 116, pp. 86–96, 2019.

[27] K. Khaledi, E. Mahmoudi, M. Datcheva, and T. Schanz, "Stability and serviceability of underground energy storage caverns in rock salt subjected to mechanical cyclic loading," *International Journal of Rock Mechanics and Mining Sciences*, vol. 86, pp. 115–131, 2016.

[28] National Standard of the People's Republic of China, *Standard for Test Method of Engineering Rock Mass. GB/T50266-2013. The Professional Standard Compilation Group of People's Republic of China*, China Planning Press, Beijing, China, 2013, in Chinese.

[29] J. Liu, H. Xie, Y. Ju et al., "Device with position-limit spring for alternating tension-compression cyclic test," Sichuan University, Chengdu, China, US Patent 9488560B2, 2016.

[30] S. Liu, J. Xu, Z. Wu et al., "Effect of strain rate on macro- and micro-structural failure characteristics of marble from split hopkinson pressure bar tests," *Géotechnique Letters*, vol. 9, no. 3, pp. 1–18, 2019.

[31] J. Lemaitre, "Evolution of dissipation and damage in metals submitted to dynamic loading," in *Proceedings of the ICM–1*, pp. 151–157, Kyoto, Japan, 1968.

[32] J. Dufailly and J. Lemaitre, "Modeling very low cycle fatigue," *International Journal of Damage Mechanics*, vol. 4, no. 2, pp. 153–170, 1995.

[33] Y. Ju and H. P. Xie, "A variable condition of the damage description based on hypothesis of strain equivalence," *Chinese Journal of Applied Mechanics*, vol. 15, no. 1, pp. 43–49, 1998, in Chinese.

[34] J.-F. Liu, Y. Bian, D.-W. Zheng, Z.-D. Wu, and T.-Y. Li, "Discussion on strength analysis of salt rock under triaxial compressive stress," *Rock and Soil Mechanics*, vol. 35, no. 4, pp. 919–925, 2014, in Chinese.

[35] Z. Hou, "Mechanical and hydraulic behavior of rock salt in the excavation disturbed zone around underground facilities," *International Journal of Rock Mechanics and Mining Sciences*, vol. 40, no. 5, pp. 725–738, 2003.